

An Aerodynamics Analysis of Rear Wing of Formula – 1 car using Eppler E423 as Wing Profile

Piyush chavda¹, Prof. Darshan Ajudia²,
Department of Mechanical Engineering^{1,2}, Marwadi Education Foundation,
FOPG, Rajkot, Gujarat, India^{1,2}
Email: M.E student- piyushchavda119@gmail.com¹, Assistant Professor-
Darshan.ajudia@marwadieducation.edu.in²

Abstract- In racing sport vehicles and Automobiles vehicles, the aerodynamics plays an important role in efficiency of the vehicle and engine performance. To maximize the performance of the vehicle, the aerodynamics forces acting on the automobile vehicle and how to utilize those forces for increasing the performances and stability. The wing or spoiler generally mounted on top of car's rear end and also positioned under the front bumper. The low pressure zone at back end creates drag force on vehicle, which is overcome by using rear Spoiler. The different designs of rear spoiler used are based on the different type of the automobile vehicles and aerofoil used. In this study, we have chosen formula-1 car spoiler with Eppler E423 aerofoil profile for our analysis purpose. To perform analysis we have used commercial software CREO and AUTOCAD for solid modeling of F1 car wing body. After that for analysis we use CFD tools – ANSYS FLUENT. By this analysis we can find out lift and drag forces, distributions of pressure and velocity. It is found that E423 is suitable for higher speed and producing more negative lift as well as more drag. So possibly we can improve aerodynamics characteristics of Formula -1 or automobile vehicles.

Index Terms- CFD analysis, Co-efficient of drag and lift, Formula 1 rear wing, Eppler E423 Aerofoil, Turbulence Analysis

1. INTRODUCTION

Formula one's racing event currently known as the FIA Formula One World Championship. Due to increasing nature of competition, changes in regulations, the ever increasing need to cut costs by reduced track testing and, maybe in the future, a freeze on design changes collectively contribute to the need of dependence on computer simulations for various aspects of performance enhancement. The aerodynamic design has two primary functions. First one, the creation of downforce to help improve the cornering force and pushes the car's tires onto the track. Second one, to minimizing the drag that caused by turbulence and shape of car body or automobile vehicle and trying to slow the car down. Due to high strength-to-weight ratio, fiber-reinforced composites are often more profitable and efficient than conventional materials. The air flow over two different sides of rear wing of aerofoil contour, have to travel different distance by different speed produces pressure difference between sides of aerofoil. This pressure difference generates the downward force to the car. This pressure can make the wing tries to move in the direction of the low pressure called negative lift in this case of aerodynamics. As flow of air over the wing, it's disturbed by the shape of aerofoil wing causing a drag force. Although this drag force generated due to shape of wing in air flow is generally less than lift or downforce.

2. LITERATURE REVIEW

Francesco Mariani et al. [1] were studied external aerodynamics of Formula SAE car racing both experimentally and as well as numerically. They have found that use of wing reduce total drag forces and increases downward forces. S.M. Rakibul Hassan et al. [2] was Numerically Studied Aerodynamic Drag Reduction of Racing Cars. Drag coefficient was found to be 0.3233. Whereas, for Rear under- body diffuser gives 9.5% drag coefficient reduction. Sneha Hetawala et al. [3] researched on Aerodynamic Study of Formula SAE Car. Drag co-efficient is reduced from 0.85 to 0.70. Negative lift is increased from 0.2 to 0.25 when having wing at front section. Overall pressure around the driver head region is dropped from 340Pa to 80 Pa when cut out made section at firewall. C.V.Karthick et al.[4] researched numerically about optimization of a car spoiler. The change in Cd with respect to the speed of the racing automobile car is negligible. The downforce acting on the racing car with the rear spoiler increases notably lower as increase in the speed of the racing car. Additionally, we get the higher Cl and Cd for lower spoiler height. Wael A. Mokhtar [5] has studied about high-lift low Reynolds numbers airfoils. It's found that E423 stall conditions are smooth and also less dependence on Reynolds number. E423 has higher camber generates higher maximum lift. Ravon Venters et al. [6] have numerically investigated high lift coefficient airfoil near region of stall. E423 airfoil the experiment

indicates that the AOA of maximum lift is between 13 and 14 degrees. The Eppler 423 airfoil gave the highest lift coefficients at $Re = 1 \times 10^6$. Xu-xia Hu et al. [7] were numerically researched for Rear spoiler Of Passenger Vehicle, Drag reductions for case 1 - 0.574 and Drag reductions for case 2 - 0.564. Development of aerodynamic in F1 cars now a day, almost all the team uses the advantages of CFD by means some CFD software packages. The results are produced without manufacturing or construction of the required F1 car and its components prototype, which is a main advantage of CFD. Analyze flow around F1 car rear wing with particular wing profile and its drag and lift generation to improve its performance.

Computational fluid dynamics (CFD) is widely used in the field of aerodynamics for design and analysis of aerospace and automobile vehicles. Different rear wing design gives different flow structure around body with respect to various parameters like speed, AOA, height, etc. In this study, we have used Solid modeling software of preparation of model and for meshing purpose ICEM CFD is used. Further, to perform analysis of rear wing of formula one car ANSYS FLUENT 17.2 was used.

3. OBJECTIVES

1. Design of aerodynamic rear wing of formula one's car with Eppler E423.
2. Analyses the drag coefficient, C_d , lift coefficient, C_l , pressure and velocity variations at different speed for the designed aerofoil.
3. with having 1 camber length height and AOA ($^\circ$) -2, 0, 2, 6, 10

4. METHODOLOGY

The model of formula one car's rear wing with Eppler E423 aerofoil is prepared with commercial software using CREO and AUTOCAD. Then various aerofoils with different angle of attack will be made with base model.

- Solver - Pressure based solver
- Time - steady flow
- Turbulence - K- ω model
- Solution methods - SIMPLE
 - Gradient - least square call based
 - Pressure - second order
 - Momentum - second order upwind
 - Turbulent kinetic energy - Second order upwind
 - Turbulent Dissipation rate - Second order upwind
- Initialization- hybrid Initialization
- Initialization iteration - 200
- Solution iteration - 750

SST k- ω turbulent model is used for these analyses. K- ω includes two extra transport equations to represent turbulent properties. K- ω model is reported to perform better in transitional flows and in flows with adverse pressure gradients. The model is numerically very stable, especially the low- Re version, as it tends to produce converged solutions more rapidly than the k - ϵ models. K- ω model predicts well near wall So SST K- ω model is selected due to combines the k - ω and K- ϵ turbulence model such that the k- ω is used in the inner region of the boundary layer and switches to the K- ϵ in the free shear flow.

5. PHYSICAL MODEL

As we mention earlier, the physical model of rear wing of formula one car is modeled with help of commercial software CREO and AUTOCAD and the profile of wing is selected as Eppler E423. Which was also generated with help of CREO modeling software as per regulations of 2018 FIA FORMULA 4 TECHNICAL REGULATIONS [8] and Data points are extracted from Eppler E423 data chart. We generated different model on the basis of different AOA.

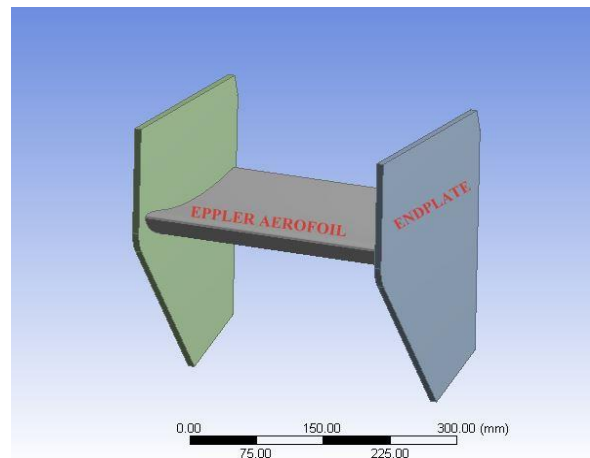


Figure 1: Isometric view of Rear wing of Formula 1 car.

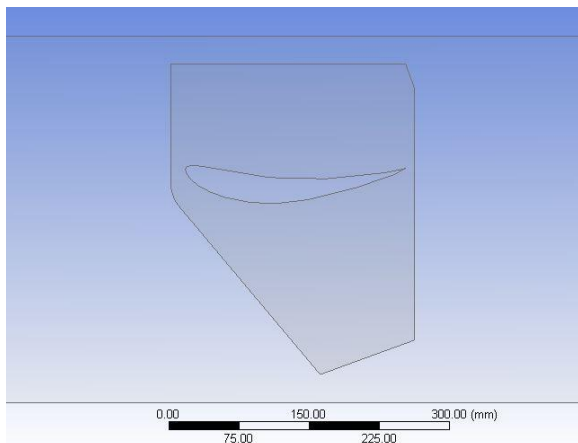


Figure 2: Side view of Rear wing of Formula 1 car.
Table-1: Dimension of rear wing of Formula 1 car.

Sr. no	Parts	Dimensions
1.	Chord of aerofoil	235 mm
2.	Maximum camber of aerofoil	22.325 mm
3.	Location of Maximum Camber from Leading edge of aerofoil	97.29 mm
4.	Maximum thickness of aerofoil	29.375 mm
5.	Height of aerofoil from ground	235 mm (1 c)
6.	Height of end Plate	300 mm
7.	Width of end plate	250 mm
8.	Wide span of Aerofoil	300 mm

6. DOMAIN SET-UP AND MESH GENERATION

Domain is main part of analysis problem. In which, we focused region of flow phenomena. We have selected domain area around rear wing to capture proper fluid flow phenomena. The size of domain is

Table-2: Dimension of Domain of rear wing of Formula 1 car.

Sr. No	Entity	Dimensions
1.	Inlet distance from leading Edge	1c (235 mm)
2.	Outlet distance from trailing edge	1c (235 mm)
3.	Domain	1235mm x 360mm x 360mm (L x B x H)

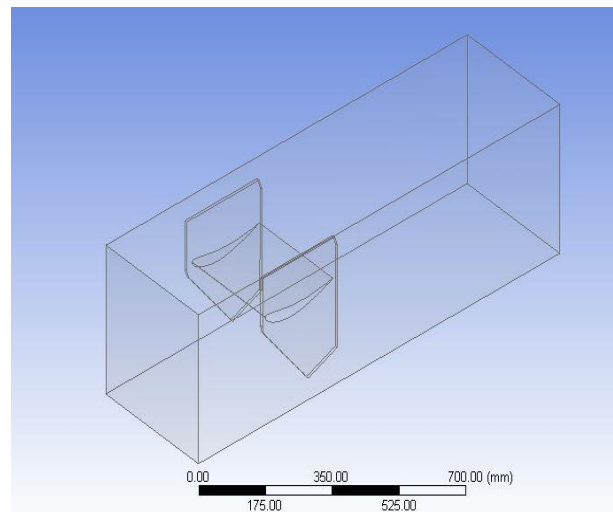


Figure- 3: Domain of Rear Wing.
The generation of mesh in domain area is done by using ICEM CFD. The generated elements are tetrahedral in nature. The mesh near to wall or periphery of aerofoil should be fine as possible to resolve and capture proper Fluid flow phenomena.

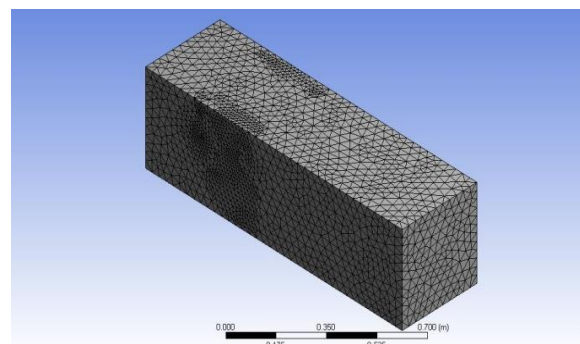


Figure- 4: Isometric view of mesh of rear wing.

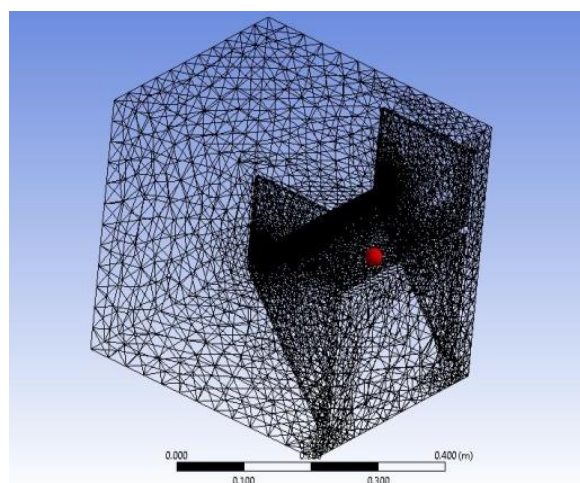


Figure- 5: Sectional view of mesh and wireframe.

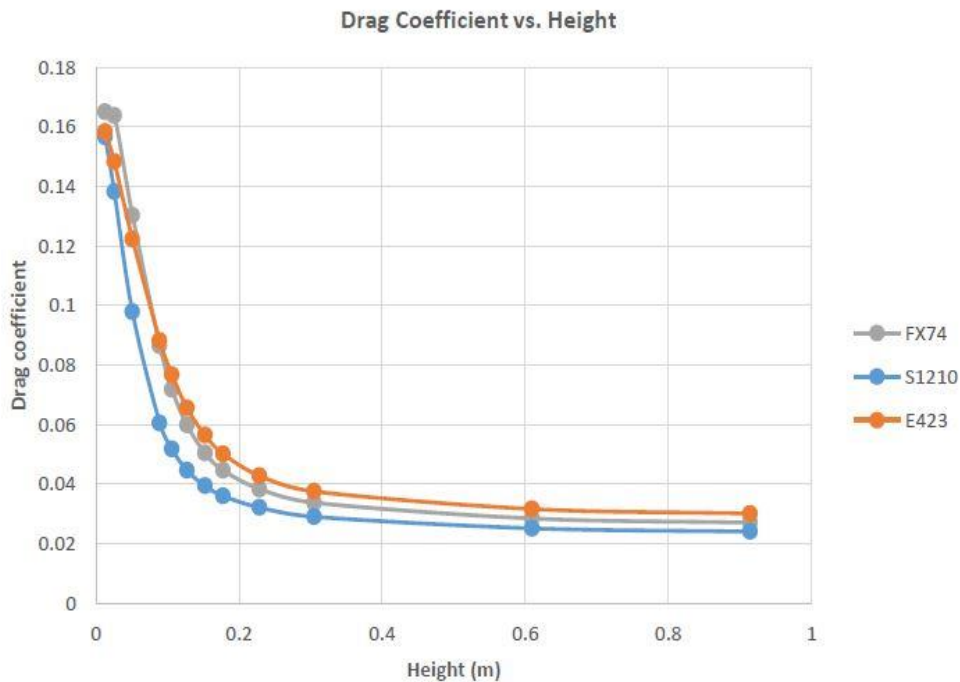


Figure – 4: Cd vs H, data of Grabis, Michael *et al.* [12]

7. GOVERNING EQUATIONS

We consider a steady, 3D incompressible flow in a rectangular domain. All fluid properties are assumed to be constant. We assume no body forces acting on body of rear wing. Under these assumptions, the 3D incompressible Navier- Stokes equations and equations of co-efficient of lift and drag are

7.1 Continuity Equation

$$\frac{\partial u}{\partial x} + \frac{\partial v}{\partial y} + \frac{\partial w}{\partial z} = 0$$

7.2 Momentum Equations

$$\rho \frac{Du}{Dt} = \rho g_x - \frac{\partial p}{\partial x} + \mu \left(\frac{\partial^2 u}{\partial x^2} + \frac{\partial^2 u}{\partial y^2} + \frac{\partial^2 u}{\partial z^2} \right)$$

$$\rho \frac{Dv}{Dt} = \rho g_y - \frac{\partial p}{\partial y} + \mu \left(\frac{\partial^2 v}{\partial x^2} + \frac{\partial^2 v}{\partial y^2} + \frac{\partial^2 v}{\partial z^2} \right)$$

$$\rho \frac{Dw}{Dt} = \rho g_z - \frac{\partial p}{\partial z} + \mu \left(\frac{\partial^2 w}{\partial x^2} + \frac{\partial^2 w}{\partial y^2} + \frac{\partial^2 w}{\partial z^2} \right)$$

7.3 Navier-Stokes Equations

$$\rho \left(\frac{\partial u}{\partial t} + u \frac{\partial u}{\partial x} + v \frac{\partial u}{\partial y} + w \frac{\partial u}{\partial z} \right) =$$

$$\rho g_x - \frac{\partial p}{\partial x} + \mu \left(\frac{\partial^2 u}{\partial x^2} + \frac{\partial^2 u}{\partial y^2} + \frac{\partial^2 u}{\partial z^2} \right)$$

$$\rho \left(\frac{\partial v}{\partial t} + u \frac{\partial v}{\partial x} + v \frac{\partial v}{\partial y} + w \frac{\partial v}{\partial z} \right) =$$

$$\rho g_y - \frac{\partial p}{\partial y} + \mu \left(\frac{\partial^2 v}{\partial x^2} + \frac{\partial^2 v}{\partial y^2} + \frac{\partial^2 v}{\partial z^2} \right)$$

$$\rho \left(\frac{\partial w}{\partial t} + u \frac{\partial w}{\partial x} + v \frac{\partial w}{\partial y} + w \frac{\partial w}{\partial z} \right) =$$

$$\rho g_z - \frac{\partial p}{\partial z} + \mu \left(\frac{\partial^2 w}{\partial x^2} + \frac{\partial^2 w}{\partial y^2} + \frac{\partial^2 w}{\partial z^2} \right)$$

7.4 Lift co-efficient

$$Cl = \frac{L}{\left(\frac{\rho V^2 A}{2} \right)}$$

7.5 Drag co-efficient

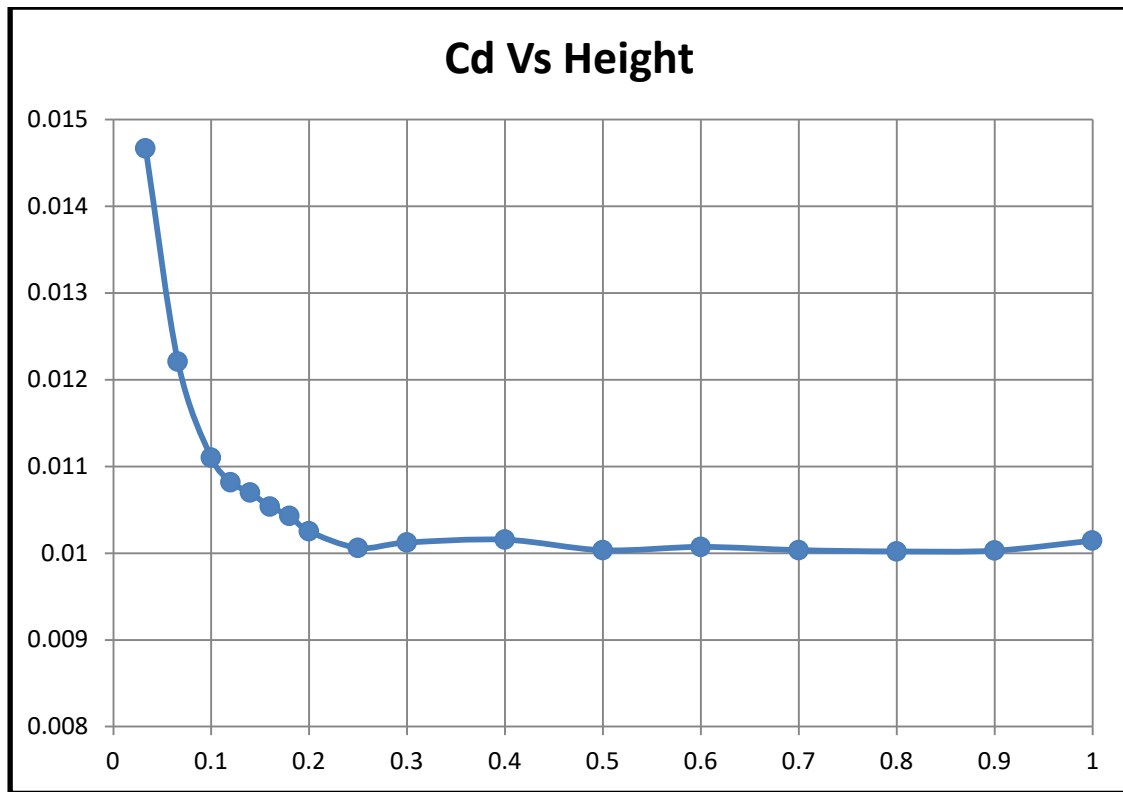


Figure – 5: Cd vs h/c of calculated data for rear wing of car (EPPLER E423)

$$Cd = \frac{D}{\frac{\rho V^2 A}{2}}$$

Table-4: Grid Dependency Test

Sr. No	Nodes	Elements	Cl	Cd
1	125522	669595	-0.077042	0.0046470
2	169272	902040	-0.076528	0.0046379
3	248233	1320859	-0.075186	0.0046298
4	358821	1905777	-0.073513	0.0045979

Grid independency test was carried out on rear wing F-1 car model with EPPLER E423 aerofoil for refinement of results. From above 2nd test having minimum percentage changes of Cl and Cd, So we choose 2nd mesh size for further analysis.

8. VALIDATIONS

The various analyses performed on model of different AOA chosen at two different speeds of 120KMPH and 180 KMPH. Different values of Cl and Cd are obtained.

A constant AOA (°) = 6 is used and the airfoil analysis are all run at the same speeds with the same chord lengths as the first study of validation and Re = 2,95,000. As from above plot (Figure-5), we get almost same fashion as Grabis, Michael *et al.* [26](Figure-4) Performed but, there is some change in value of Cd at different ground clearance. This happens due to we have done analysis in 3- dimensional geometry.

9. RESULTS AND DISCUSSION

Results of EPPLER E423 at 120 KMPH

Table-5: Cl and Cd w.r.t Different AOA At 120 KMPH of EPPLER E423

AOA	Cl	Cd
-2	-0.060835	0.0037507
0	-0.076528	0.0046379
2	-0.091957	0.0057775
6	-0.12105	0.0089413
10	-0.14971	0.013122

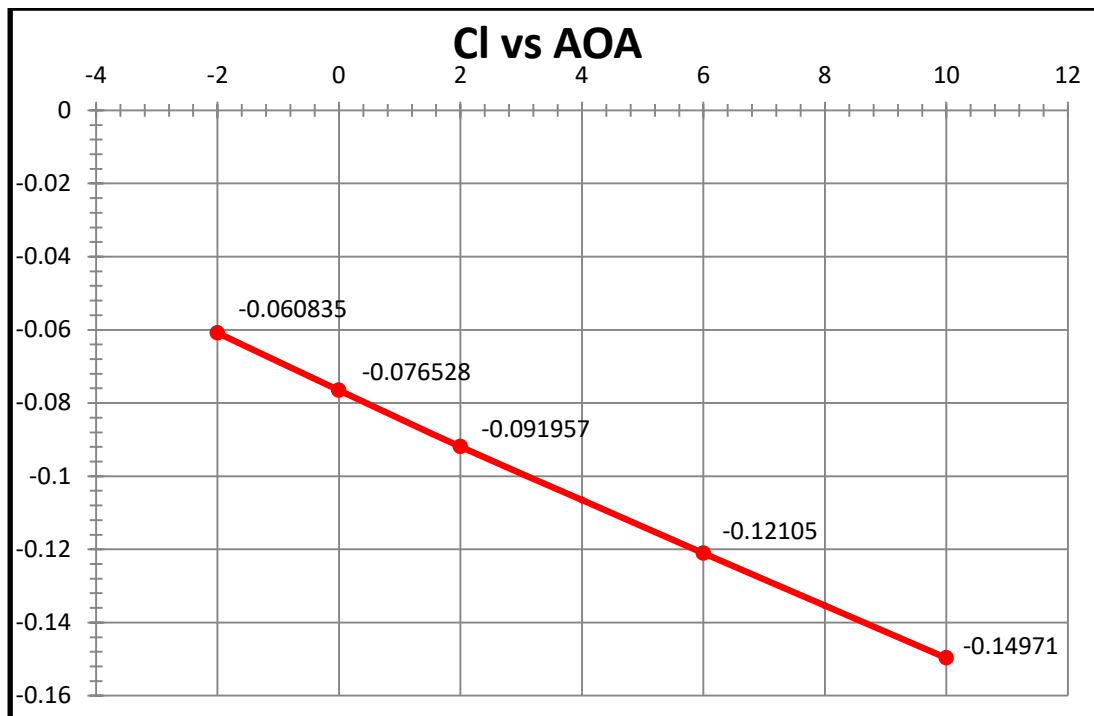


Figure – 6: Value of Cl vs. different AOA at 120 KMPH of EPPLER E423

From calculated data for EPPLER E423 aerofoil at different AOA at 120 KMPH, It shows that there is steady increase in Negative lift of rear wing of F1 car. The fashion is observed in negative co-efficient of lift, Cl w.r.t increase in AOA (°) -2 to 10. The values of negative Cl are steadily increases from -0.060835 to -0.14971. There is increment in valve of co-efficient of drag, Cd from 0.0037507 to 0.013122, when AOA (°) are changes from -2 to 10.

0	-0.077098	0.0045577
2	-0.092411	0.0057358
6	-0.12179	0.0088875
10	-0.15072	0.013106

From calculated data for EPPLER E423 aerofoil at different AOA at 180 KMPH, It shows that there is steady increase in Negative lift of rear wing of F1 car. The fashion is observed in negative co-efficient of lift, Cl w.r.t increase in AOA (°) -2 to 10. There is also increment in valve of co-efficient of drag, Cd from 0.0036508 to 0.013106, when AOA (°) are changes from -2 to 10.

Results of EPPLER E423 at 180 KMPH

Table- 6: Cl and Cd w.r.t Different AOA At 180 KMPH of EPPLER E423

AOA	Cl	Cd
-2	-0.061416	0.0036508

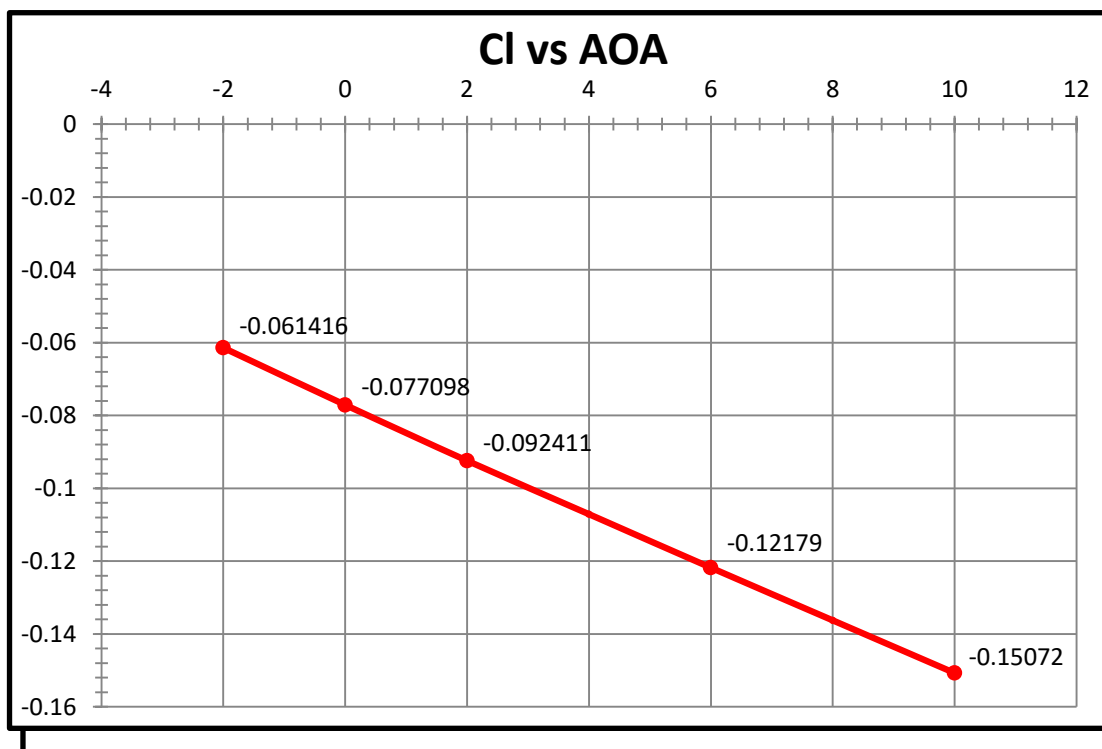


Figure – 9: Value of Cl vs. different AOA at 180 KMPH of EPPLER E423

Figure – 7: Value of Cd vs. different AOA at 120 KMPH of EPPLER E423

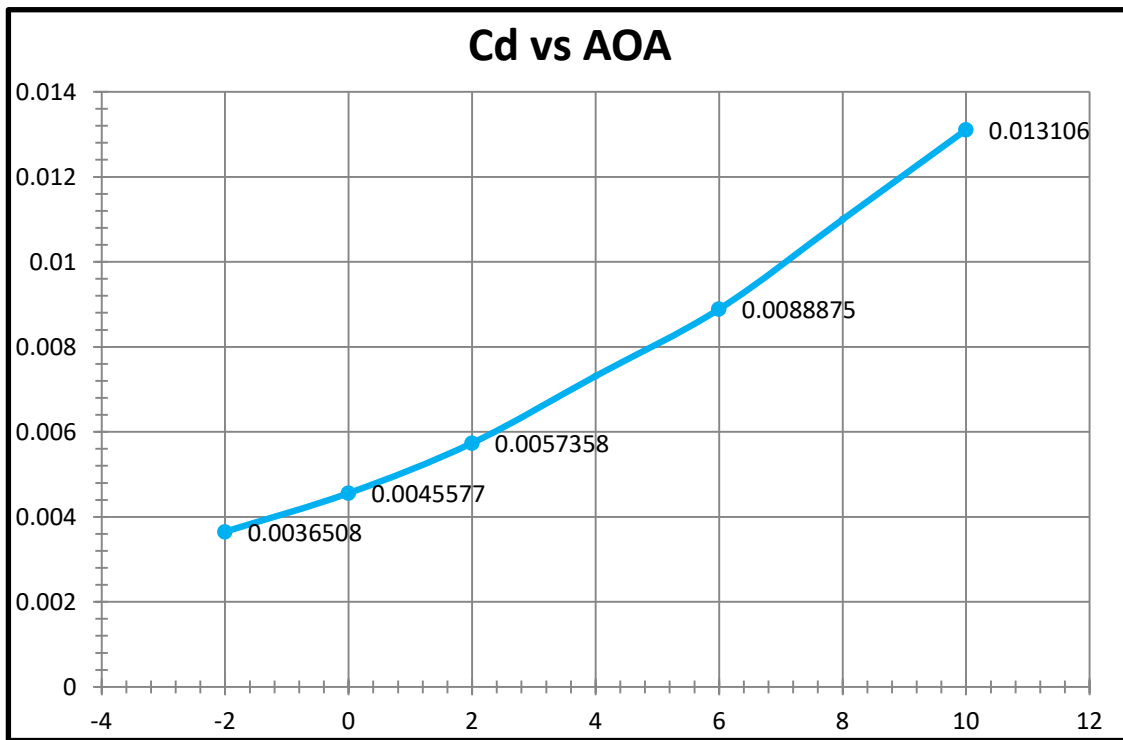


Figure – 10: Value of C_d vs. C_l of 180 KMPH of EPPLER E423

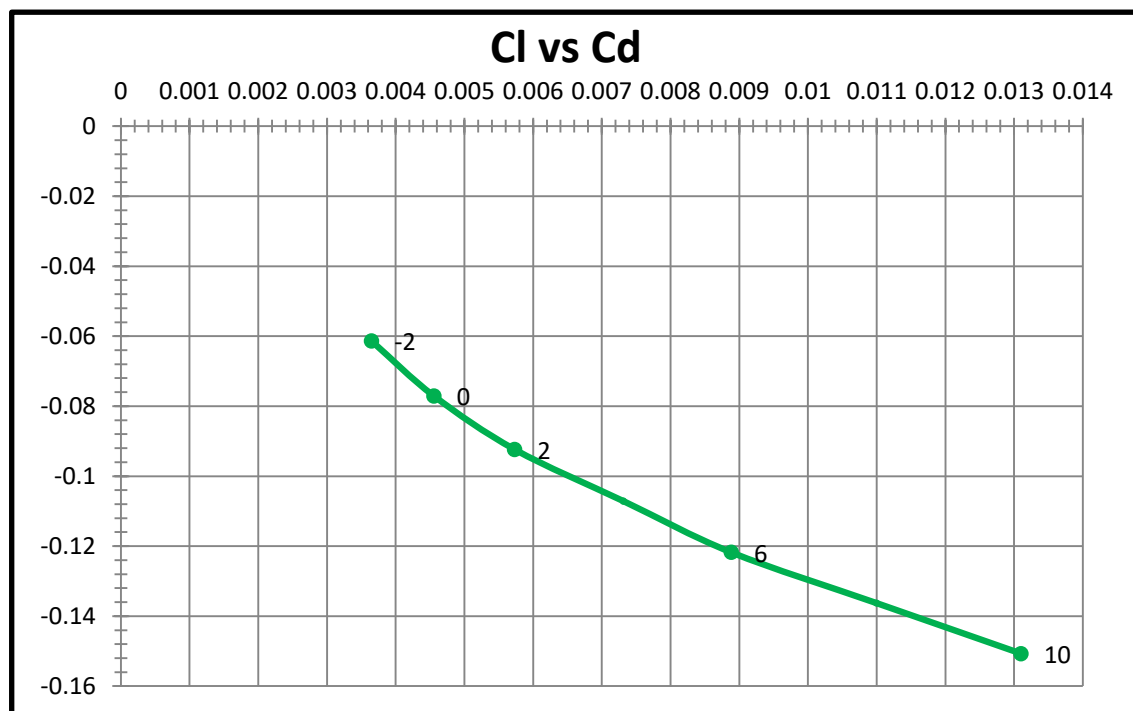


Figure – 11: Cd vs. C_l of 180 KMPH of EPPLER E423

From figure 12 and 14, the stagnation point shifts bottom to top on leading edge as AOA ($^{\circ}$) changes to -2 to 10. The small lower pressure zone exists at AOA ($^{\circ}$) is equal to -2 and 0. There is big lower pressure zone observed at bottom side of aerofoil, when AOA ($^{\circ}$) changes to -2 to 10. The Spoiler resists the flow of the Fluid passing on the airfoil, which creates the drag force to be increased. The frontal projected area of airfoil to the flow of fluid is gradually increased when AOA ($^{\circ}$) changes from -2 to 10. This fashion observed at both speed of car (120 KMPH, 180 KMPH) for different AOA ($^{\circ}$) = -2 to 10 of Eppler E423 airfoil profile. But EPPLER E423 airfoil generates higher negative lift at 180 KMPH than 120 KMPH and generates lower drag at 180 KMPH than 120 KMPH.

There is two high velocity zone seen in velocity distribution contours. The two high velocity zones are present – smaller and larger. The small high velocity zone is at top side of airfoil and near leading edge (Figure 13 and 15). The size of small high velocity zone exists when AOA ($^{\circ}$) is equal to -2 to 0, the small high velocity zone vanishes at AOA ($^{\circ}$) = 2. The big high velocity zone always present at bottom side of airfoil. There is also two low velocity zone see in velocity distribution contours. The two low velocity zones are present – smaller and larger. The smaller lower velocity zone is present near at leading edge of airfoil and also it shift from bottom side of airfoil to top side of airfoil as AOA ($^{\circ}$) changes to -2 to 10. The small low velocity zone is merges to big low velocity zone at AOA ($^{\circ}$) is equal to 10. The big small velocity zone is seen as AOA ($^{\circ}$) changes to -2 to 10. Also there is low velocity zone found behind the airfoil. It can be seen that the air flow behind the spoiler is being disturbed. This low velocity zone produces drag and negative effect to negative lift of rear wing of car. The growth of low velocity zone behind the airfoil is increases as AOA ($^{\circ}$) changes to -2 to 10. It clearly indicates that the velocity in the lower side increases with increase in AOA. This fashion observed at both speed of car(120 KMPH, 180 KMPH) for different AOA ($^{\circ}$) = -10 to 10 of EPPLER E423 airfoil profile.

- EPPLER E423 airfoil produces higher negative lift C_L at higher speed of F1 car.
- EPPLER E423 airfoil produces lower drag C_d at higher speed of F1 car.
- EPPLER E423 airfoil produces higher lift C_L as AOA is increases.
- EPPLER E423 airfoil is suitable for higher speed of F1 car due to its produces lower drag C_d as well as higher negative lift C_L .

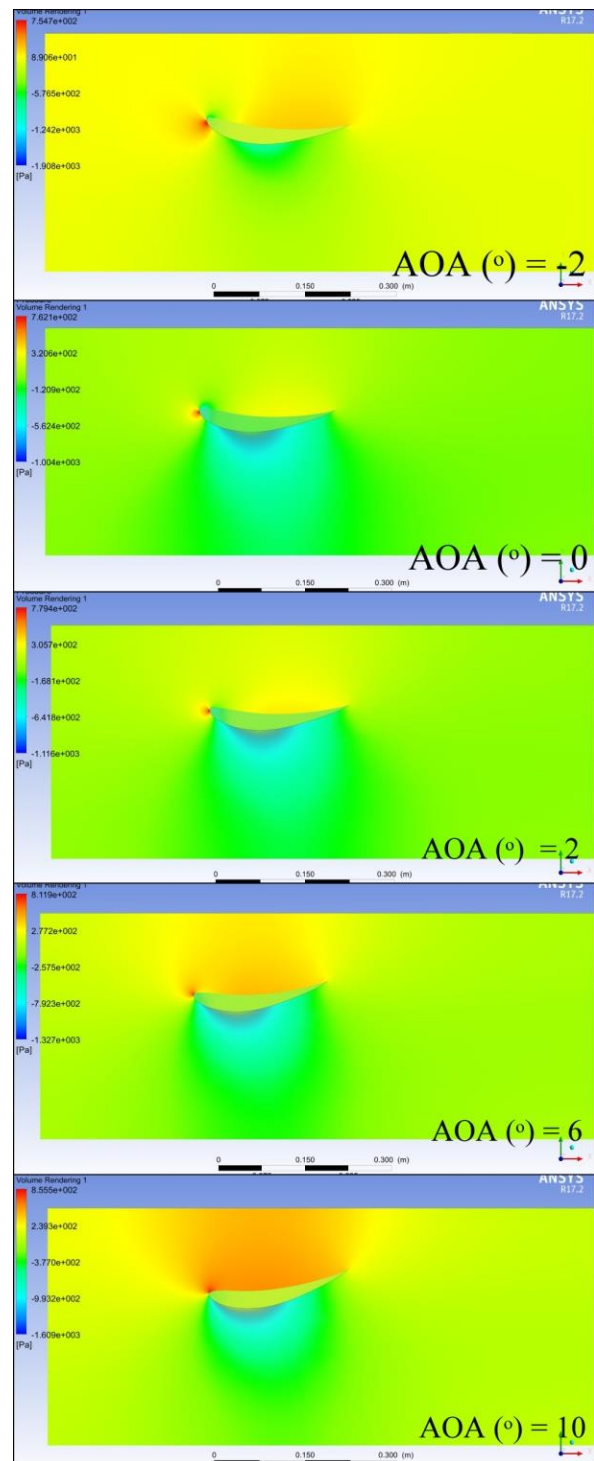


Figure – 12: Pressure Contours of 120 KMPH of EPPLER E423

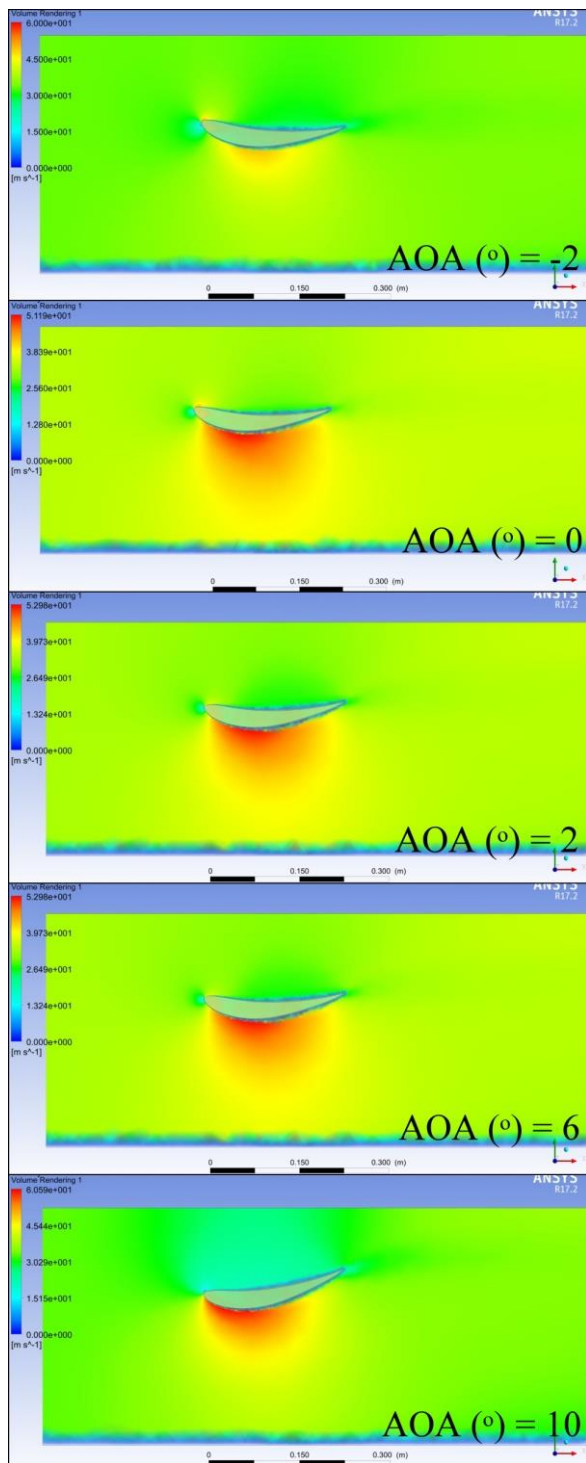


Figure – 13: Velocity Contours of 120 KMPH of EPPLER E423

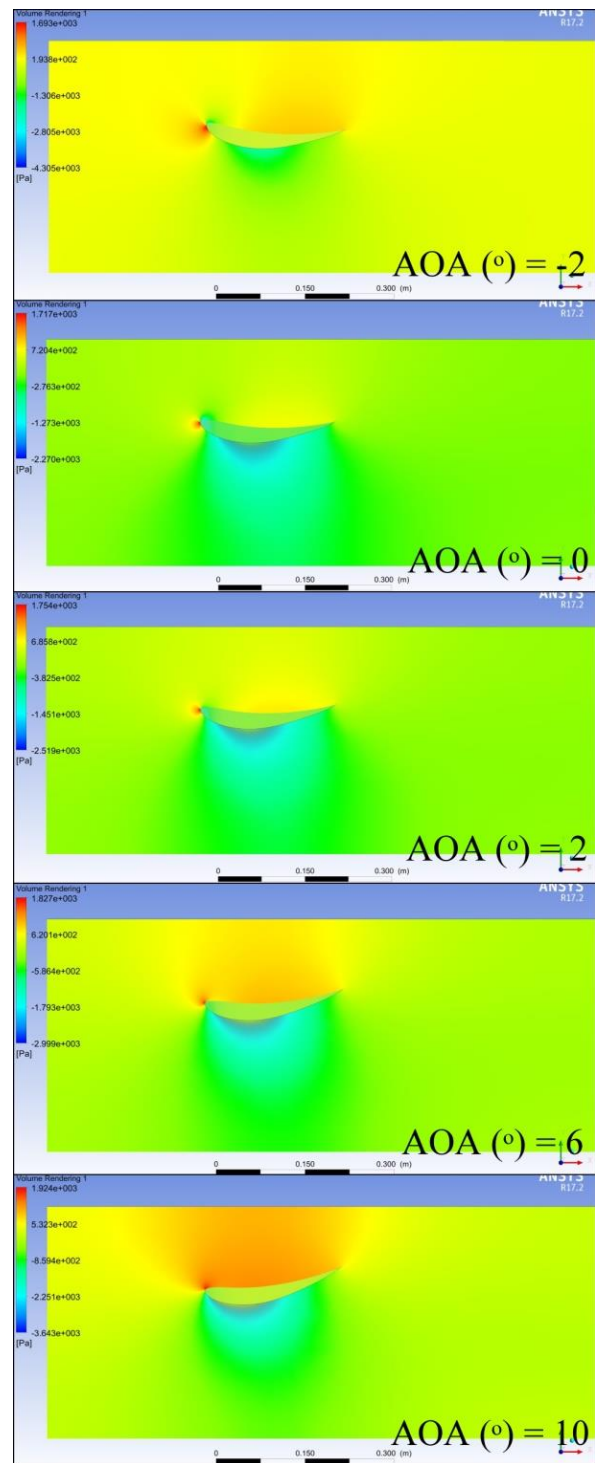


Figure – 14: Pressure Contours of 180 KMPH of EPPLER E423

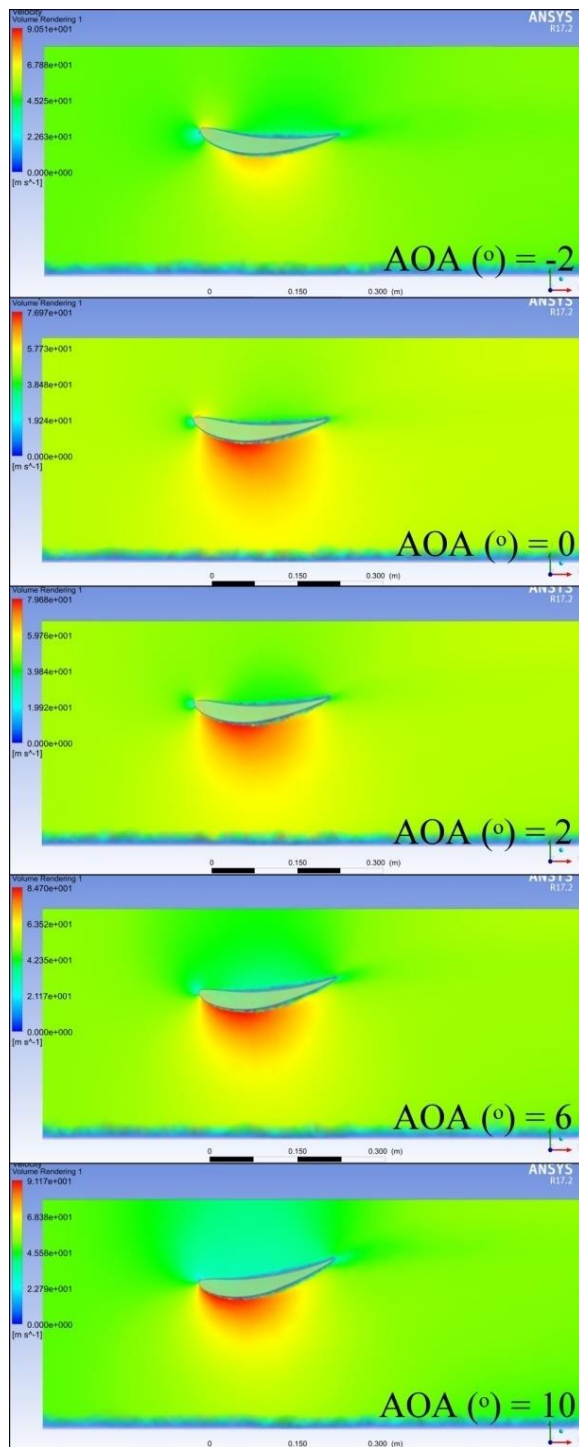


Figure – 15: Velocity Contours of 180 KMPH of EPPLER E423

10. CONCLUSIONS

Computational analysis using ANSYS FLUENT to predict flow around Rear wing of race car has been achieved. 3-D external flows around the rear wing of formula one car were investigated. In this study, three

parameters were taken into consideration, AOA, speed of car, Eppler E423 Aerofoil. By comparing the results of various cases of different AOA and speed of car, we can get information about aerodynamics of Formula one car. The aerodynamic of racing cars can be improved by use of computational fluid dynamics. The set of results and observations included in this paper suggests that CFD can be a very useful tool to support the aerodynamic design of race cars.

REFERENCES

- [1] Francesco Mariani, Claudio Poggiani, Francesco Risi, Lorenzo Scappaticci “Formula SAE car racing: Experimental and numerical analysis of the external aerodynamics” ELSEVIER-Energy Procedia, Volume 81, December 2015, Pages 1013-1029
- [2] S.M. Rakibul Hassan, Toukir Islam, Mohammad Ali, Md. Quamrul Islam “Numerical Study on Aerodynamic Drag Reduction of Racing Cars” ELSEVIER – Procedia Engineering Volume 90, 2014, Pages 308-313
- [3] Sneha Hetawala, Mandar Gophaneb, Ajay B.K.c, Yagnavalkya Mukkamalad “Aerodynamic Study of Formula SAE Car” ELSEVIER - Procedia Engineering Volume 97, 2014, Pages 1198-1207
- [4] C.V.Karthick, Bala Murugan, P.A.Nigal Ashik, P.Raju “CFD Analysis and Optimization of a Car Spoiler” Research India Publications - International Journal of Mechanical Engineering and Research, ISSN 0973-4562 Vol. 5 No.1 (2015)
- [5] Wael A. Mokhtar “A Numerical Parametric Study of High-Lift Low Reynolds Number Airfoils” 43rd AIAA Aerospace Sciences Meeting and Exhibit, 10 – 13 January 2005, Reno, Nevada
- [6] Ravon Venters and Brian Helenbrook “A numerical investigating of high lift coefficient airfoils near regions of stall” Proceedings of the ASME 2013 Fluids Engineering Division Summer Meeting, FEDSM2013 July 7-11, 2013, Incline Village, Nevada, USA
- [7] Xu-xia Hu, Eric T.T. Wong “A Numerical Study On Rear-spoiler Of Passenger Vehicle” World Academy of Science, Engineering and Technology 57 2011
- [8] A.Muthuvel, N. Prakash , J. Godwin John “Numerical Simulation of Drag Reduction in Formula One Cars” International Journal of Engineering Research and Applications (IJERA), March – 2014, ISSN: 2248-9622.
- [9] B.Navin kumar , K.M.Paramasivam , M.Prasanna A.Z.G Mohamet Karis “Computational Fluids Dynamics of Aerodynamics Characteristics NACA 4412 VS S809 Airfoil for Wind Turbine Applications” International Journal of Advanced Engineering Technology, Sept-2016 E-ISSN 0976-3945.

- [10] Piyush Chavda, Darshan Ajuida “Computational Analysis of Aerodynamics Effects of a Rear Wing/Spoiler of Formula –1Car.”International Journal of Engineering Research in Mechanical and Civil Engineering (IJERMCE) Vol 3, Issue 4, April 2018
- [11] Grabis, Michael and Agarwal, Ramesh K. “Computational Fluid Dynamics Analysis of High Lift, Single Element, Inverted Airfoils in Ground Effect for an FSAE Car Front Wing”. Mechanical Engineering and Materials Science Independent Study 2017 – 59

APPENDIX

Cl = Co-efficient of Lift

Cd = Co-efficient of drag

AOA = Angle of Attack

ν = The Effective Viscosity or Turbulent eddy viscosity

τ_{ij} = The shear-stress tensor.

P = Pressure of Fluid

u = Velocity of Fluid in x direction.

ρ = Density of Fluid

K = Turbulent Kinetic Energy

ϵ = Rate of dissipation of Kinetic Energy

ω = The Specific Rate of Dissipation

d = The Distance from the field point to the nearest wall

F = Additional Functions